

## **Modeling of Gas Phase Transport and Composition Evolution during the Initial Stage Sintering of Boron Carbide with Carbon Additions**

M. A. Rossi, M. J. Matthewson<sup>\*†</sup>, A. Kaza<sup>‡</sup>, D. Niesz<sup>†</sup>, R. A. Haber<sup>†</sup>

Department of Materials Science and Engineering

Rutgers, The State University of New Jersey

607 Taylor Road, Piscataway, New Jersey 08854

### **Abstract**

Densification of  $B_4C$  during sintering can be aided by removing the native  $B_2O_3$  (condensed) layer present on the starting  $B_4C$  powder.  $B_2O_3$  can be removed by adding excess C and holding the powder compact at an intermediate temperature below the normal sintering temperature. This allows time for CO and minor boron gases to diffuse out from the porous compact before the pores close. This process is examined using a computational model based on co-diffusion of multiple gas species, which enables prediction of the gas and condensed phase composition as a function of time and position in the specimen. The model, previously described elsewhere, was originally applied to the SiC/SiO<sub>2</sub> system but has been adapted for the  $B_4C/B_2O_3$  system. The results are used to determine the optimum holding time for complete  $B_2O_3$  (condensed) removal as a function of key parameters, such as specimen thickness, particle size, temperature, *etc.* The role of gas phase transport in residual C and  $B_4C$  profiles is also examined.

\*Communicating author's e-mail: mjohnm@fracture.rutgers.edu

†Fellow of the American Ceramic Society

‡Current affiliation: Intel Corporation, Portland Oregon

## I. Introduction

Lee and Speyer<sup>1</sup> suggest that reduced densification during pressureless sintering of  $B_4C$  without sintering agents may be due to the presence of a  $B_2O_3(c)$  film on  $B_4C$  particles.<sup>1,2</sup> The  $B_2O_3$  film prevents direct contact between  $B_4C$  particles (and a resulting increase in densification) and acts as a rapid diffusion path at large particle surfaces, facilitating particle coarsening.<sup>1,3</sup> The addition of SiC,  $Al_2O_3$ ,  $TiB_2$ ,  $AlF_3$  and  $W_2B_5$  have been used to enhance densification, but has caused grain growth.<sup>3</sup> The removal of the  $B_2O_3(c)$  coating permits direct  $B_4C$  particle contact, and an increase in densification.<sup>3</sup> The addition of C aids the removal of the  $B_2O_3(c)$ .<sup>1-3</sup> This is analogous to what occurs in the SiC system,<sup>4-7</sup> in which it is thought that one of the factors leading to high density SiC is the complete removal of the  $SiO_2$  oxide layer at temperatures lower than typical sintering temperatures.

The amount of C added to the starting  $B_4C$  powder is important because there must be enough C for complete  $B_2O_3(c)$  reduction, to prevent low final densities, while C inclusions from an excess C content will lead to a deterioration of mechanical properties.<sup>1</sup> The holding time at a particular temperature is also critical – sufficient holding time must be provided to remove all  $B_2O_3(c)$ ; however, a longer holding time leads to grain coarsening and a less efficient heating cycle.<sup>1-3</sup>

The  $B_2O_3$  is removed via the gas phase and so gas diffusion is the rate determining step for complete removal of  $B_2O_3$ . The purpose of the current work is to model the gas diffusion to determine the needed hold time as a function of key parameters such as temperature, pore size, *etc.*, as well as to examine the spatial variation in residual  $B_4C$  and C content after complete removal of  $B_2O_3(c)$ .

## II. The Model

Thermodynamic data have been obtained for the various gas species that are present in the  $B_4C/C/B_2O_3(c)$  system.<sup>8-10</sup> Figure 1 shows the partial pressure of several gas species

in equilibrium with the starting composition of  $B_4C$ , C and  $B_2O_3(c)$ , as a function of temperature. Many species have an extremely small partial pressure in the temperature range of interest ( $\sim 1200$  to  $2500$  K); thus, they have a negligible impact on the rate of mass transport in the gas phase and so can be safely ignored in the modeling.

The removal of  $B_2O_3(c)$  from the  $B_4C/C/B_2O_3$  system in the presence of trace chemical species, such as those present as contaminants (*e.g.*,  $H_2O$ ), is not considered in this paper. The underlying assumption is that the model is operating in ideal vacuum conditions and at high temperatures. We therefore assume that any species that are volatile at lower temperatures will have already been removed – this includes water.

$B_4C$  is well-known to exhibit carbon deficient non-stoichiometry over a broad range of composition. Non-stoichiometric  $B_4C$  will consume free carbon and must be stoichiometric with unit activity in the presence of pure carbon (also unit activity).<sup>13</sup> Therefore, extra carbon is needed to avoid incomplete  $B_2O_3(c)$  removal. The additional quantity can be calculated from the starting  $B_4C$  stoichiometry; provided the necessary extra carbon is added, the non-stoichiometry of the starting  $B_4C$  does not impact the ability of the carbon to remove  $B_2O_3(c)$ .

### (1) The Gas Diffusion Model

The model considers the diffusion of four gas species through the specimen pores. These include CO, the most abundant gas,  $B_2O_2$  and  $B_2O_3(g)$  which are the most abundant gases containing B and BO.  $O_2$  is also considered even though its pressure is very low in this system, because it is a convenient vehicle for calculations.

This situation is analogous to sintering of SiC. In that system, the native  $SiO_2$  can also impede densification and can be removed by the addition of C. The oxygen is removed primarily by effusion of CO, although the minor species SiO is important for controlling interparticle neck growth. In previous work<sup>11</sup> we describe a detailed model for multiple species gas co-diffusion to examine how gas partial pressures and condensed

phase composition varies with time and position inside an SiC body. The model is used to determine how the hold time needed for complete  $\text{SiO}_2$  removal depends on key parameters.

This model has been adopted for use with the  $\text{B}_4\text{C}-\text{C}-\text{B}_2\text{O}_3$  system. Some adaptations are simple, such as using appropriate thermodynamic data and molecular diameter data. However, some aspects of the computational model required significant changes, including complete changes of the stoichiometric coefficients (which are hard-coded in the computer program for efficiency). Also, there is only one significant Si containing gas in the SiC system (*i.e.* SiO) whereas there are three in the  $\text{B}_4\text{C}$  system ( $\text{B}_2\text{O}_2$ ,  $\text{B}_2\text{O}_3$ , BO). The reader is referred to Kaza, *et al.* for details of the computational model.<sup>11</sup> Here we limit ourselves to outlining where the model for  $\text{B}_4\text{C}$  differs significantly from the SiC model.

The problem is modeled using a finite difference method where a one-dimensional body (large plate) is divided into a finite number of nodes and the composition at each node and diffusion between adjacent nodes are calculated over a series of time steps. Various boundary conditions can be applied to the free surface. In this work we assume the body is exposed to vacuum so that any gas flowing out is immediately removed.

The model assumes that the composition of the gas phase at each node is locally always in equilibrium with the condensed phases. At each time step, gases can diffuse into or out of each node at a rate given by the Dusty Gas Model (DGM). The DGM implementation used in the model is due to Mason and Malinauskas<sup>12</sup> and incorporates three mechanisms: Knudsen diffusion, continuum or inter-diffusion, and diffusion due to viscous flow. Knudsen diffusion involves gas molecule-pore wall interactions. Inter-diffusion accounts for the interaction between the multiple gas species, while the diffusion due to viscous flow arises from pressure gradients in the gas mixture.

The gases are replenished by adjusting condensed species composition at each node. As in the SiC model, two distinct thermodynamic regimes of interest can be identified. In

Regime 1, all three condensed phases are present,  $B_4C$ ,  $C$ ,  $B_2O_3(c)$ , while in Regime 2 the  $B_2O_3(c)$  has been completely exhausted. Equilibrium conditions are calculated differently for each regime.

## (2) Thermodynamics

### *Regime 1*

In this regime, the determination of equilibrium gas partial pressures can be performed directly because there are three condensed phases (Note that, depending on the temperature, the standard state of  $B_2O_3$  (condensed) can be either solid or liquid since the melting point is 723 K) and three atomic species. As a result, any gas species can be expressed in terms of the condensed species alone

$$CO(g) = \frac{1}{3} B_2O_3(c) + \frac{7}{6} C(s) - \frac{1}{6} B_4C(s) \quad (1)$$

$$B_2O_2(g) = \frac{2}{3} B_2O_3(c) - \frac{1}{6} C(s) + \frac{1}{6} B_4C(s) \quad (2)$$

$$B_2O_3(g) = B_2O_3(c) \quad (3)$$

$$BO(g) = \frac{1}{3} B_2O_3(c) - \frac{1}{12} C(c) + \frac{1}{12} B_4C(c) \quad (4)$$

$$O_2(g) = \frac{2}{3} B_2O_3(c) + \frac{1}{3} C(c) - \frac{1}{3} B_4C(c) \quad (5)$$

The standard free energy change for each of the above reactions is determined by summing the free energies of the individual species. The equilibrium constant can be calculated and expressed in terms of the activities. For CO

$$K_{CO} = \exp\left(-\frac{\Delta G_{CO}^\circ}{RT}\right) = \frac{a_{B_2O_3}^{1/3} a_C^{7/6} a_{B_4C}^{-1/6}}{p_{CO}} \quad (6)$$

Assuming the condensed species have unit activity (pure), this gives the partial pressure of CO ( $p_{CO}$ ) directly

$$p_{\text{CO}} = \exp\left(\frac{\Delta G_{\text{CO}}^{\circ}}{RT}\right) \quad (7)$$

The partial pressures of the other gas species are calculated in an analogous fashion. The assumption of unit activity of the condensed species is made for the sake of simplicity. Therefore, the model used for this work does not account for the well-known non-stoichiometry that  $\text{B}_4\text{C}$  can exhibit<sup>13,14</sup> but assumes that the  $\text{B}_4\text{C}$  has consumed enough of the free carbon to become stoichiometric, as described earlier.

### *Regime 2*

In Regime 2, the calculation of equilibrium gas partial pressures can not be performed explicitly because oxygen is absent from the condensed phases. However, they can be expressed in terms of the condensed species and any oxygen containing gas;  $\text{O}_2$  has been used for convenience

$$\text{CO(g)} = 0.5 \text{O}_2\text{(g)} + \text{C(s)} \quad p_{\text{CO}} = p_{\text{O}_2}^{1/2} K_{\text{CO}}^{-1} \quad (8)$$

$$\text{B}_2\text{O}_2\text{(g)} = 0.5\text{B}_4\text{C(s)} + \text{O}_2\text{(g)} - 0.5\text{C(s)} \quad p_{\text{B}_2\text{O}_2} = p_{\text{O}_2} K_{\text{B}_2\text{O}_2}^{-1} \quad (9)$$

$$\text{B}_2\text{O}_3\text{(g)} = 1.5\text{O}_2\text{(g)} + 0.5\text{B}_4\text{C(s)} - 0.5\text{C(s)} \quad p_{\text{B}_2\text{O}_3} = p_{\text{O}_2}^{3/2} K_{\text{B}_2\text{O}_3}^{-1} \quad (10)$$

$$\text{BO(g)} = 0.25 \text{B}_4\text{C(s)} + 0.5 \text{O}_2\text{(g)} - 0.25 \text{C(s)} \quad p_{\text{BO}} = p_{\text{O}_2}^{1/2} K_{\text{BO}}^{-1} \quad (11)$$

The additional constraint needed to solve these simultaneous equations is mass balance; namely that the quantity of each atomic species does not change as the system maintains equilibrium at every region as the various gases diffuse in or out of a particular region. It is sufficient to only consider oxygen. The total number of moles of oxygen atoms (*i.e.* g-atoms of oxygen) is given by

$$n_{\text{O}} = A \left( p_{\text{CO}} + 3p_{\text{B}_2\text{O}_3} + 2p_{\text{B}_2\text{O}_2} + p_{\text{BO}} + 2p_{\text{O}_2} \right), \quad (12)$$

where  $A$  is a factor that converts from gas partial pressure (in atmospheres) to number of moles, taking into account the properties of an ideal gas, the volume associated with the

region under consideration, and the porosity. Substituting in terms of  $p_{\text{O}_2}$  from equations (8) to (11), gives

$$n_{\text{O}} = A \left( p_{\text{O}_2}^{1/2} K_{\text{CO}} + 3 p_{\text{O}_2}^{3/2} K_{\text{B}_2\text{O}_3} + 2 p_{\text{O}_2} K_{\text{B}_2\text{O}_2} + p_{\text{O}_2}^{1/2} K_{\text{BO}} + 2 p_{\text{O}_2} \right). \quad (13)$$

The equation constants are again found from thermodynamic data. Conservation of O requires the solution of a cubic equation in  $p_{\text{O}_2}^{1/2}$  (compared with a quadratic equation for the SiC system).

### (3) Conservation of Matter

Once the gas phase composition is adjusted to maintain local equilibrium, the composition of the condensed phase is adjusted to maintain overall conservation of matter. This is assumed to occur rapidly so that reaction kinetics are not rate determining. This assumption was justified for the SiC system for which density gradients are observed in sintered SiC bodies of size  $\sim 1$  cm (which would not be observed if reaction kinetics were rate controlling). This assumption will also be valid for  $\text{B}_4\text{C}$  for sufficiently large bodies. However, gas diffusion will be rapid in very small bodies and so in that case reaction kinetics will be rate controlling. The model here will therefore only be valid for  $\text{B}_4\text{C}$  bodies above some size. Unfortunately there are no data available in the literature for reaction kinetics, so it is not possible to explicitly find where the rate controlling process changes. However, it is clear that the longer the required time for complete  $\text{B}_2\text{O}_3$  removal, the less likely that reaction kinetics are controlling.

The change in the quantity of each condensed species is calculated using the reactions given in equations (1) to (5). For example, in Regime 1, the change in the number of moles of each solid is given by

$$\delta n_{\text{C}} = -\frac{7}{6} \delta n_{\text{CO}} + \frac{1}{6} \delta n_{\text{B}_2\text{O}_2} + \frac{1}{12} \delta n_{\text{BO}} - \frac{1}{3} \delta n_{\text{O}_2}, \quad (14)$$

$$\delta n_{\text{B}_4\text{C}} = \frac{1}{6} \delta n_{\text{CO}} - \frac{1}{6} \delta n_{\text{B}_2\text{O}_2} - \frac{1}{12} \delta n_{\text{BO}} + \frac{1}{3} \delta n_{\text{O}_2}, \quad (15)$$

$$\delta n_{\text{B}_2\text{O}_3} = -\frac{1}{3} \delta n_{\text{CO}} - \frac{2}{3} \delta n_{\text{B}_2\text{O}_2} - \delta n_{\text{B}_2\text{O}_3} - \frac{1}{3} \delta n_{\text{BO}} - \frac{2}{3} \delta n_{\text{O}_2} . \quad (16)$$

The coefficients in each equation are the stoichiometric coefficients for the corresponding solid in equations (1) to (5) with the sign changed to recognize that if the stoichiometric coefficient is positive, that amount of solid decreases when the amount of gas increases. Similar results are obtained for Regime 2 using equations (8) to (10).

$$\delta n_{\text{C}} = -\delta n_{\text{CO}} + 0.5 \delta n_{\text{B}_2\text{O}_3} + 0.5 \delta n_{\text{B}_2\text{O}_2} + 0.25 \delta n_{\text{BO}} , \quad (17)$$

$$\delta n_{\text{B}_4\text{C}} = -0.5 \delta n_{\text{B}_2\text{O}_3} - 0.5 \delta n_{\text{B}_2\text{O}_2} - 0.25 \delta n_{\text{BO}} . \quad (18)$$

#### (4) Reference Modeling Conditions

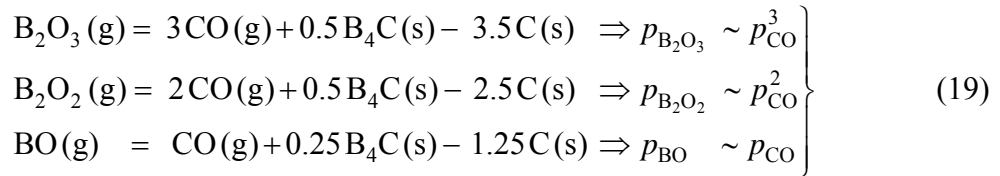
Table I describes a set of “reference” parameter values that are in the range typical of values encountered when sintering  $\text{B}_4\text{C}$  parts. The reference case represents the conditions described by Dole *et al.*,<sup>15</sup> for samples prepared with a 6 wt% C addition. The effect of varying the parameters from this reference case has been studied.

### III. Results and Discussion

#### (1) Results for the “Standard” Case

Figures 2 to 4 show how the gas pressures and condensed phase composition vary with time and position through the thickness of the body for the reference conditions specified in Table I. Initially, all gases are set to the equilibrium partial pressure for an isothermal temperature of 1640 K. There is no driving force for diffusion except at the specimen surface. As time progresses, the gasses diffuse out from the surface, gradually exhausting the  $\text{B}_2\text{O}_3$ (c). It can be seen that  $\text{B}_2\text{O}_3$ (c) is exhausted first at the region near the surface and last near the center. An abrupt interface separates the two regions. A reaction front therefore propagates into the body corresponding to the position where the system is changing from Regime 1 to Regime 2. Here, the quantity of  $\text{B}_2\text{O}_3$  is decreasing with time. The interior of the specimen is in Regime 1, and has the starting composition. The partial pressures in this region do not change with time, so there is negligible driving

force for diffusion until the reaction front arrives, explaining the flat-topped pressure profiles observed in figures 2 and 3. The region nearer the surface is in Regime 2 and is exhausted of  $B_2O_3(c)$ . CO is the dominant gas species and so dominates the diffusion kinetics. The total amount of CO evolved from a small region is much larger than the volume of the pores in that region. Therefore, the reaction front moves slowly and quasi-static conditions are approximately maintained. Thus, the pressure profile for CO while in Regime 2 is approximately that for steady state Fickian diffusion in one dimension, namely the pressure decreases linearly from the equilibrium regime 1 pressure at the reaction front to zero at the surface. The partial pressures of the other gas species are primarily controlled by CO, due to its abundance. Therefore, their pressure profiles are controlled by the constraint of local equilibrium rather than by the rate of diffusion. The equilibrium between these gases and CO can be examined using the following reactions; noting that only  $B_4C$  and C are present in the solid phase in Regime 2



This explains why, for a linear CO profile, the  $B_2O_2(g)$  and  $B_2O_3(g)$  profiles are curved while the BO profile is linear (Figure 3).

When the reaction front reaches the center of the sample,  $B_2O_3(c)$  is completely exhausted everywhere and this corresponds to the time for complete removal,  $t_c$ . For the “reference” case,  $t_c = 961$  s. The behavior of the C concentration is the same except that there is some residual carbon, since excess carbon is included in the starting composition to ensure complete removal of  $B_2O_3(c)$  everywhere.

If the time for complete  $B_2O_3(c)$  removal is short compared with the time to heat the  $B_4C$  through the temperature range of interest ( $\sim 1600$ - $1800$  K) then the kinetics of CO removal would not be important since the heating cycle naturally provides sufficient

time. Our reference state needs ~15 minutes for complete  $B_2O_3$  (c) removal so that gas diffusion is probably not rate controlling. However, the reference condition is chosen somewhat arbitrarily. Other reasonable parameter values can give very much longer times (*e.g.* for plates much thicker than 1 cm and for smaller grain/pore sizes). So the model is still useful because it can be used to determine whether an intermediate hold time is needed, and, if it is needed, how long it should be.

## (2) Influence of Parameter Values on Hold Time for Complete $B_2O_3$ Removal

The model has been used to investigate the effect of the various parameters on the time needed for complete  $B_2O_3$  (c) removal. These studies involve holding all parameters the same as in the “reference” case defined in Table I except for the parameter of interest.

Figures 5 to 10 show the effect of the various parameters on holding time,  $t_c$ . Many of these parameters will be related in a particular material – changing grain size, porosity, pore size *etc.* will all change surface area and so change the quantity of  $B_2O_3$  present. However, we do not in advance know the relationship between these parameters for any given specimen – they must be measured. Once measured, parameter values of interest can be used for input to the model. Since none of the parameters used by the model are artificially coupled in any way, its general applicability is conserved. These parameters are hard to measure and it is unrealistic that they should be measured for every specimen. However, the model is useful since it shows what trends are expected to be seen as the various parameters change.

In the present work, three gases act to deplete B from  $B_2O_3$ , leading to the need for more complex mathematical relationships to describe system behavior than required by the SiC system. However, since the resulting difference in behavior is very slight, it is thought that the simple relationships previously developed for the SiC system are acceptable here.<sup>11</sup> Table II describes the influence of each parameter on the holding time for depletion of  $B_2O_3$  in the  $B_4C$  system.

### (3) Semi Empirical Equation for the Holding Time

The dependence of holding time on an individual parameter such as sample thickness, pore size, porosity *etc.* is described in table II. In all cases, the dependence of  $t_c$  on each parameter can be put in a linearized form by finding an appropriate function of the parameter. Using the example of porosity, the model finds that  $t_c$  varies approximately linearly with  $(1-\varepsilon)/\varepsilon$  for reasons that are explained in Reference 11. This results in an equation of the form  $t_c = t_0(1 + b_\varepsilon \Delta[(1-\varepsilon)/\varepsilon])$  where  $\Delta[(1-\varepsilon)/\varepsilon]$  is the change in  $(1-\varepsilon)/\varepsilon$  going from the reference state to the conditions of interest. The coefficient  $b_\varepsilon$  is the slope of a straight line fitted to  $t_c$  as a function of  $(1-\varepsilon)/\varepsilon$  and describes the sensitivity of  $t_c$  to this parameter. Table II shows these linearized forms for all the parameters under consideration, together with their coefficients.

Assuming that the dependencies of  $t_c$  on the various parameters are weakly coupled, the dependence of  $t_c$  when multiple parameters are varied simultaneously can be described by combining the equations given in table II

$$t_c = t_0 \left( 1 + b_\varepsilon \Delta \left[ \frac{1-\varepsilon}{\varepsilon} \right] \right) \cdot \left( 1 + b_r \Delta \left[ \frac{1}{r} \right] \right) \cdot (1 + b_q \Delta[q]) \quad (20)$$

$$\times \left( 1 + b_l \Delta[l^2] \right) \cdot \left( 1 + b_{X_{B_2O_3}} \Delta[X_{B_2O_3}] \right) \exp(-b_T \Delta[T])$$

The amount by which each parameter is varied gives an idea of how sensitive  $t_c$  is to that parameter. The model has been run for the case where all parameters are simultaneously adjusted by the amounts shown in Table III. Under these circumstances, if the  $t_c$  for each parameter were doubled, *i.e.*  $t_c = 2.0t_0$ , equation (20) predicts that  $t_c$  would be increased to  $64t_0 = 17.09$  hr; the model gives a value of 18.44 hr. This shows that the coupling between the individual parameters is weak, so that equation (20) makes good predictions of  $t_c$  even when the parameters are changed by a large amount. Equation (20) can be used to provide guidance for the needed holding time, even for conditions where the

parameters deviate significantly from the values in Table I, thus obviating the need to run the computer model for every set of experimental parameters.

In this context, “coupling” refers to the extent to which the various parameters interact within the dusty gas model. In practice, the values of the parameters will be extrinsically coupled by other considerations – as already mentioned, changing the porosity, pore size *etc.* will change the amount of  $B_2O_3$  which contaminates the particle surfaces. Such extrinsic coupling will likely be strong. However, we show here that the intrinsic coupling of the parameters within the dusty gas model is weak.

#### (4) Spatial Variation of Final Composition

##### *Spatial Variation in $B_2O_3$ Content*

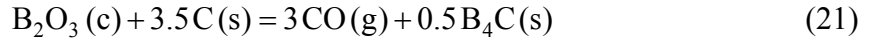
As mentioned,  $B_2O_3$  is detrimental to the densification of  $B_4C$  due to the occurrence of non-densifying mechanisms<sup>1-3</sup> such as grain coarsening.<sup>15</sup> The results presented here show that the depletion of  $B_2O_3$  begins near the surface and ends at the specimen center (figure 4). If the hold time is less than  $t_c$ , the interior region will contain more  $B_2O_3$  than regions near the surface. This suggests that density gradients could arise after sintering, with regions near the surface exhibiting higher densities. This prediction is supported by the observation of less grain coarsening near the surface of a  $B_4C$  specimen fired without added carbon; this was attributed to removal of  $B_2O_3$  by volatilization from the surface.<sup>15</sup>

The time needed for complete  $B_2O_3$  removal ( $t_c$ ) obviously depends on the starting  $B_2O_3$  content. In this work, the amounts of carbon and  $B_2O_3$  were adjusted to coincide with a particular experimental case.<sup>15</sup> The starting  $C/B_2O_3$  ratio (under the “standard” conditions described in table I) is 20.9, which is more than enough to ensure complete  $B_2O_3$  removal throughout the body while maintaining sufficient carbon to ensure the  $B_4C$ -C system remains stoichiometric.

### *Spatial Variation in C and B<sub>4</sub>C Content*

In the previous work on the SiC-C-SiO<sub>2</sub> system<sup>11</sup> there were minor variations in the final solid composition across the thickness of the SiC body. This was a minor effect caused by the diffusion of SiO out of the interior region of the solid compact; this SiO partially reacts with remnant carbon nearer the surface thus depleting the carbon near the surface slightly more than near the center. Similar effects have been found for the B<sub>4</sub>C system but they are more pronounced because the ratio of the  $p_{B_xO_y}$  (primarily B<sub>2</sub>O<sub>2</sub> and B<sub>2</sub>O<sub>3</sub> and a small amount of BO) to  $p_{CO}$  is greater than the ratio of  $p_{SiO} / p_{CO}$  in the SiC system - more oxygen is transported out of the body in species other than CO in the B<sub>4</sub>C system. This results in a significant compositional variation across the thickness of the final B<sub>4</sub>C body that could have practical importance.

Figure 11(a) shows the residual C as a function of position after complete removal of B<sub>2</sub>O<sub>3</sub> at  $t_c$ . As mentioned, more C is consumed near the surface due to reaction with B<sub>x</sub>O<sub>y</sub> gases. The oxygen in condensed (liquid) B<sub>2</sub>O<sub>3</sub> is removed primarily via CO. Rearranging equation (1) gives



suggesting that 3.5 moles of C are required to remove each mole of B<sub>2</sub>O<sub>3</sub>. However, the reaction with additional B<sub>x</sub>O<sub>y</sub> gases perturbs this value. Figure 11(b) uses the data from 11(a) to determine the amount of C consumed for each mole of B<sub>2</sub>O<sub>3</sub> as a function of position. While on average about 3.5 moles of C are needed, nearly 4 moles are needed at the surface in order to avoid complete consumption of C, which in turn would lead to loss of stoichiometry of the B<sub>4</sub>C.<sup>13,14</sup> Therefore, under the “standard” conditions defined in Table I, the minimum necessary C/B<sub>2</sub>O<sub>3</sub> ratio is slightly less than four. For a uniform starting distribution of carbon, the final distribution is necessarily non-uniform; excess carbon must be added to ensure there is sufficient carbon throughout the volume of the

body. Figure 11(b) suggests how the starting profile of C composition can be manipulated to produce a more uniform final C profile.

The C/B<sub>2</sub>O<sub>3</sub> ratio is determined for a uniform starting composition. In practice, any variability in composition will mean more carbon needs to be added, so there is enough locally for complete B<sub>2</sub>O<sub>3</sub>(c) removal throughout the specimen. The influence of local composition fluctuations is the subject of a future paper.

The distribution of residual C for a starting uniform distribution can be examined as a function of all the key variables examined above. Figure 12(a) shows the effect of temperature ( $T$ ) on the residual C profile at  $t_c$ . Increasing  $T$  leads to larger C distribution gradients. Figure 12(b) shows the corresponding final distribution of B<sub>4</sub>C – in regions where more C is consumed, more B<sub>4</sub>C is deposited. This effect could have negative practical implications. If the additional B<sub>4</sub>C preferentially deposits in the interparticle necks, it could impede later densification by reducing the surface energy driving force. This spatial distribution of deposited B<sub>4</sub>C might lead to density gradients in the final sintered body. This mechanism is similar to a mechanism discussed by Lee and Speyer (2003) in which evaporation/condensation at higher temperature impedes densification.<sup>1</sup>

Figures 13(a-f) show how the final distribution of C varies with the other key model parameters. The only effect of pore size,  $r$ , and tortuosity,  $q$  in the model is to change the permeability and hence the gas fluxes. Since we have assumed local thermodynamic equilibrium, the amount of C consumed in a given interval of time is proportional to the flux of the B<sub>x</sub>O<sub>y</sub> gases, which are in turn related to the flux of CO (since their relative pressures are constrained by thermodynamics). The time for complete B<sub>2</sub>O<sub>3</sub>(c) removal is inversely proportional to the flux of CO, so a lower flux means a lower rate of C consumption but a proportionately longer time available for consumption. The total amount of C consumed is proportional to flux times time, thus the overall effect cancels resulting in a residual C distribution that is insensitive to these parameters. Similar arguments hold for the variation of residual carbon with specimen thickness, but only

when the results are graphed versus position normalized to the specimen thickness (Figure 13(f)). This is perhaps surprising given the common experience that variations through the specimen thickness for a variety of phenomena tend to be exaggerated for thicker specimens.

The C distribution does depend on the porosity,  $\epsilon$ , (Figure 13(b)) but this is because, in addition to its influence on the gas flux, it also controls the amount of  $B_2O_3$ (c) that needs to be removed. In this case the difference in C concentration between the center and the surface is the same. The C distribution also depends on the mole fraction of  $B_2O_3$  ( $X_{B_2O_3}$ ) (Figure 13(c)) for the same reason.

The difference in shape of the residual C profile, as characterized by the height  $y$  (figure 13(c)) is simply a multiple of  $X_{B_2O_3}$ . For example, the difference between  $X_{B_2O_3} = 0.275\%$  and  $X_{B_2O_3} = 3.3\%$  is 12. Thus, the curvature represented by  $y_3 = 12y_1$ , similarly,  $y_3 = 3y_2$ .

#### IV. Conclusions

The elimination of  $B_2O_3$  from  $B_4C$  compacts is known to be important since the presence of  $B_2O_3$  during sintering can degrade the properties of the final material.<sup>1-3</sup> One method of removing  $B_2O_3$  is to add carbon which converts it to  $B_4C$  and CO gas during heating to the sintering temperature. However, sufficient time must be given for the CO to diffuse out of the compact in order to avoid the CO pressure damaging the specimen at higher temperature. A computational model describing the diffusion of multiple gas species through a porous compact was utilized to predict the isothermal holding time needed for complete  $B_2O_3$  removal during the pre-sintering purge phase. The dependence of holding time on various parameters has been studied.

The quantities of solid and gas species were monitored as a function of time and position across the sample thickness. It was found that a reaction front travels from the surface towards the center of the sample with  $B_2O_3$  exhaustion taking place at the

reaction front. The time required for complete removal of  $B_2O_3$  therefore corresponds to the time taken for the reaction front to reach the center of the specimen.

A semi empirical equation has been developed to describe how the holding time varies with all the influencing parameters. This equation was found to represent the model well even when several parameters are varied simultaneously.

The need to minimize gradients in the final distribution of carbon, as well as of  $B_4C$ , is justified due to the role these parameters have in final density and coarsening. It was found that high temperature as well as high initial  $B_2O_3$  content leads to larger gradient in the carbon and  $B_4C$  composition. The results are qualitatively consistent with previously published experimental observations.

## V. References

- <sup>1</sup>H. Lee and R. F. Speyer, "Pressureless Sintering of Boron Carbide," *J. Am. Ceram. Soc.*, **86** [9] 1468-1473 (2003).
- <sup>2</sup>H. Lee and R. F. Speyer, "Sintering of Boron Carbide Heat-Treated with Hydrogen," *J. Am. Ceram. Soc.*, **85** [8] 2131-2133 (2002).
- <sup>3</sup>N. Cho, K. G. Silver, Y. Berta, R. F. Speyer, N. Vanier, C. H. Hung, "Densification of carbon-rich boron carbide nanopowder compacts," *J. Mater. Res.*, **22** [5] 1354-1359 (2007).
- <sup>4</sup>W. J. Clegg, "Role of Carbon in the Sintering of Boron-Doped Silicon Carbide," *J. Am. Ceram. Soc.*, **83** [5] 1039-1043 (2000).
- <sup>5</sup>S. Prochazka and R. M. Scanlan, "Effect of Boron and Carbon on Sintering of SiC," *J. Am. Ceram. Soc.*, **58** [1] 72 (1975).
- <sup>6</sup>M. Raczka, G. Gorney, L. Stobierski, K. Rozniatowski, "Effect of Carbon Content on the Microstructure and Properties of Silicon Carbide-Based Sinters," *Mater. Charact.*, **46**, 245-249 (2001).
- <sup>7</sup>L. Stobierski and A. Gubernal, "Sintering of Silicon Carbide: I. Effect of Carbon," *Ceram. Int.*, **29**, 287-292 (2003).
- <sup>8</sup>*NIST Chemistry WebBook*, National Institute of Standards and Technology. Gaithersburg MD 20899, <http://webbook.nist.gov/> 2005.
- <sup>9</sup>M. W. Chase and others, *JANAF Thermochemical Tables*. 3rd ed.; American Institute of Physics, New York, 1986. Vol. 1-2.
- <sup>10</sup>*TAPP 2.2*, version 2.2; E.S. Microware Inc.: 2234 Wade Court, Hamilton, OH 45013, <http://www.esm-software.com/> 1992.
- <sup>11</sup>A. Kaza, M. J. Matthewson, D. Niesz, R. L. Haber, M. A. Rossi, "A Model of Gas Phase Transport During the Initial Stages of Sintering of Silicon Carbide," *J. Am. Ceram. Soc.*, *in review.*, (2009).
- <sup>12</sup>E. A. Mason and A. P. Malinauskas, *Gas Transport in Porous Media; the Dusty-Gas Model*. Elsevier, Amsterdam, Netherlands, 1983.
- <sup>13</sup>D. Emin, "Structure and single-phase regime of boron carbides," *Phys. Rev. B*, **38** [9] 6041-6055 (1988).
- <sup>14</sup>L. Levin, N. Frage, M. P. Dariel, "A novel approach for the preparation of B<sub>4</sub>C-based cermets," *Int. J. Refract. Met. Hard Mater.*, **18** [2-3] 131-135 (2000).

<sup>15</sup>S. L. Dole, S. Prochazka, R. H. Doremus, "Microstructural Coarsening During Sintering of Boron Carbide," *J. Am. Ceram. Soc.*, **72** [6] 958-966 (1989).

## VI. Figure Captions

**Fig. 1:** Gas pressures as a function of temperature for several species in equilibrium with solid  $B_4C$ , C and liquid ( $T > 723$  K)  $B_2O_3$ .

**Fig. 2:** (a) Partial pressure of CO as a function of position at several times and (b) as a function of time at several positions beneath the specimen surface.

**Fig. 3:** Partial pressure profiles of the gaseous species (a)  $B_2O_2$ , (b)  $B_2O_3(g)$  and (c) BO as a function of position across the sample thickness at various times.

**Fig. 4:** (a) The profiles of  $B_2O_3(c)$  and (b) C as a function of position at various times during the temperature hold.

**Fig. 5:** Holding time for complete  $B_2O_3(c)$  removal as function of  $(1 - \varepsilon)/\varepsilon$ .

**Fig. 6:** The holding time required for the removal of  $B_2O_3(c)$ , as a function of pore radius on a reciprocal scale.

**Fig. 7:** The holding time required for the removal of  $B_2O_3(c)$ , as a function of pore tortuosity.

**Fig. 8:** The holding time required for the removal of  $B_2O_3(c)$ , as a function of the square of the specimen thickness.

**Fig. 9:** Holding time as a function of initial  $B_2O_3(c)$  content in  $B_4C$  powder.

**Fig. 10:** Holding time required for the removal of  $B_2O_3(c)$ , as a function of temperature on a semi-log scale.

**Fig. 11:** (a) Residual C concentration profile after complete  $B_2O_3$  depletion from specimen. (b) Change in number of moles of C normalized to the initial number of moles of  $B_2O_3$ .

**Fig. 12:** (a) Residual C concentration profile at  $t_c$ , as a function of temperature ( $T$ ). (b) Change in  $B_4C$  concentration profile at  $t_c$ , as a function of temperature ( $T$ ).

**Fig. 13:** Residual C concentration profile at  $t_c$  as a function of (a) pore radius  $r$ , (b) porosity  $\varepsilon$ , (c)  $X_{B_2O_3}$ , (d) tortuosity  $q$ , and (e) specimen thickness,  $l$ . (f) shows the data from (e) re-graphed as a function of position normalized to the overall specimen thickness.

## Tables

**Table I:** Parameter values used for the reference simulation.<sup>15</sup>

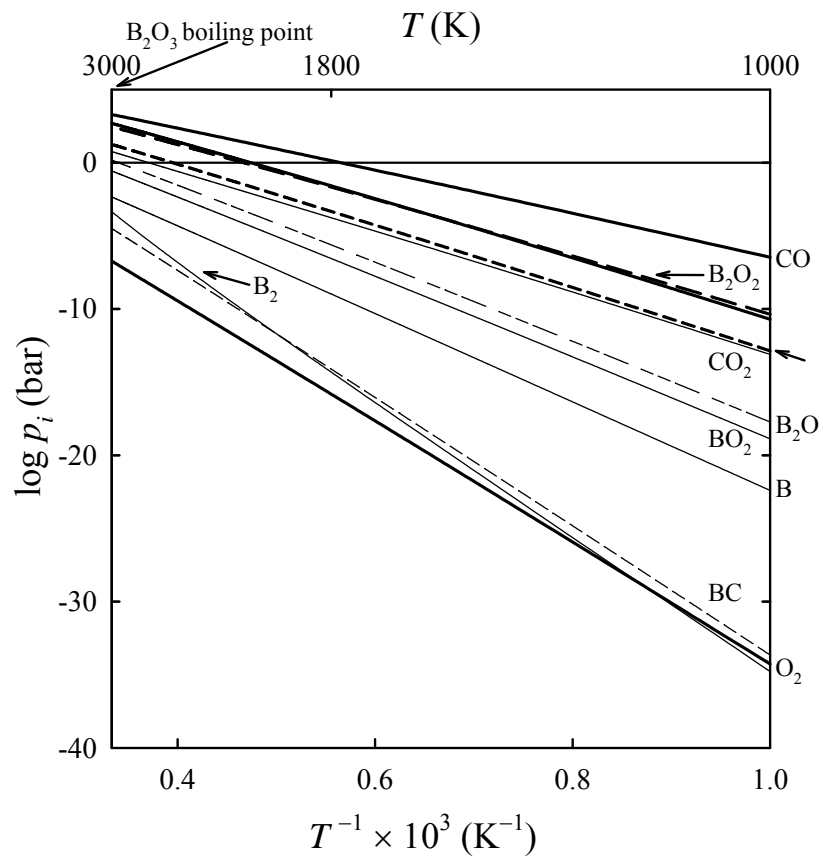
specimen thickness ( $l$ )	10 mm
pore radius ( $r$ )	70 nm
porosity ( $\varepsilon$ )	0.4
tortuosity ( $q$ )	5
mole fraction of carbon ( $X_C$ )	23.0%
mole fraction of $B_2O_3$ ( $X_{B_2O_3}$ )	1.1%
temperature ( $T$ )	1640 K
external environment	vacuum

**Table II:** Linearized equations relating time for complete  $B_2O_3(c)$  removal,  $t_c$ , to each parameter.  $t_c$ ; takes a value of  $t_0 = 0.267$  hr for the standard conditions listed in Table I.

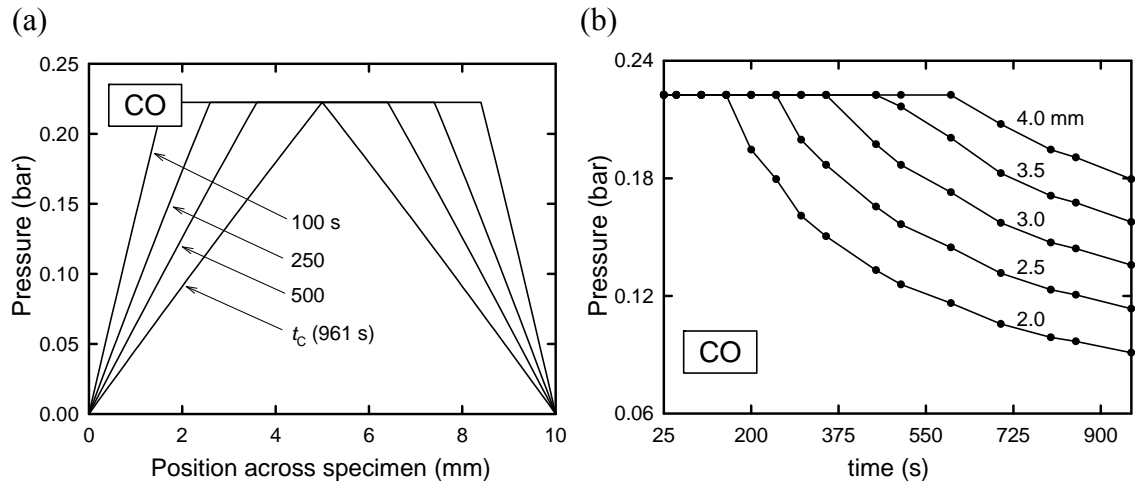
Parameter	Expression for $t_c$	$b_i$
porosity ( $\varepsilon$ )	$t_0(1 + b_\varepsilon \Delta[(1 - \varepsilon) / \varepsilon])$	0.668
pore radius ( $r$ )	$t_0(1 + b_r \Delta[1 / r])$	69.8 nm
tortuosity ( $q$ )	$t_0(1 + b_q \Delta[q])$	0.200
specimen thickness ( $l$ )	$t_0(1 + b_l \Delta[l^2])$	$0.010 \text{ mm}^{-2}$
mole fraction ( $X$ )	$t_0(1 + b_{X_{B_2O_3}} \Delta[X_{B_2O_3}])$	0.899
temperature ( $T$ )	$t_0 \exp(-b_T \Delta[T])$	$0.011 \text{ K}^{-1}$

**Table III:** Semi-empirical equation sensitivity test.

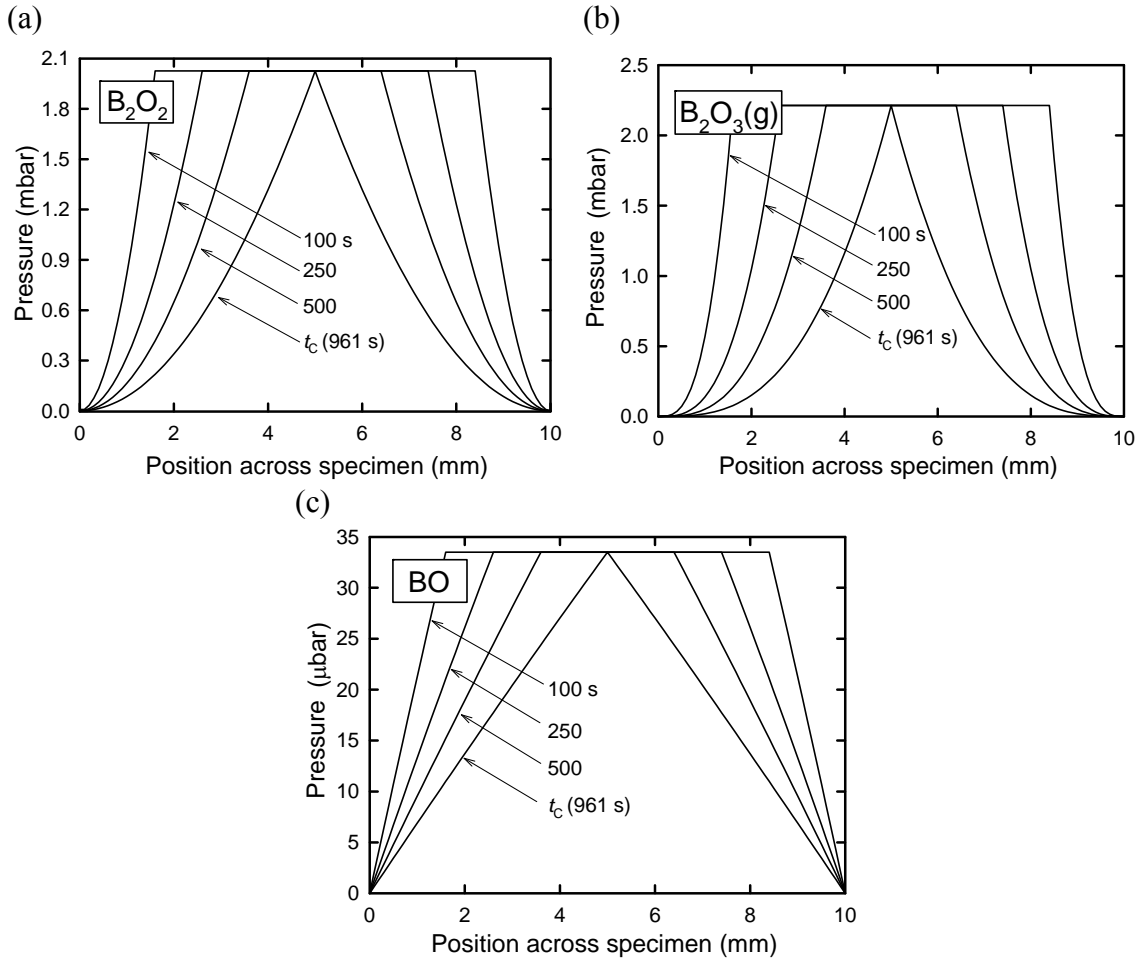
Parameter	Reference value	$1.25t_0$	$2.0t_0$	$5.0t_0$
specimen thickness ( $l$ )	10 mm	11.2 mm	14.1 mm	22.4 mm
pore radius ( $r$ )	70 nm	56.0 nm	34.9 nm	13.9 nm
porosity ( $\epsilon$ )	0.4	0.348	0.250	0.118
tortuosity ( $q$ )	5	6.25	10	25
mole fraction of $B_2O_3$ ( $X_{B_2O_3}$ )	1.1%	1.29%	2.12%	5.46%
Temperature ( $T$ )	1640 K	1620 K	1577 K	1494 K
$t_c$ predicted by model	0.267 hr	0.983 hr	18.44 hr	5902 hr
$t_c$ from Eqn. (20)	0.267 hr	1.018 hr	17.09 hr	4172 hr



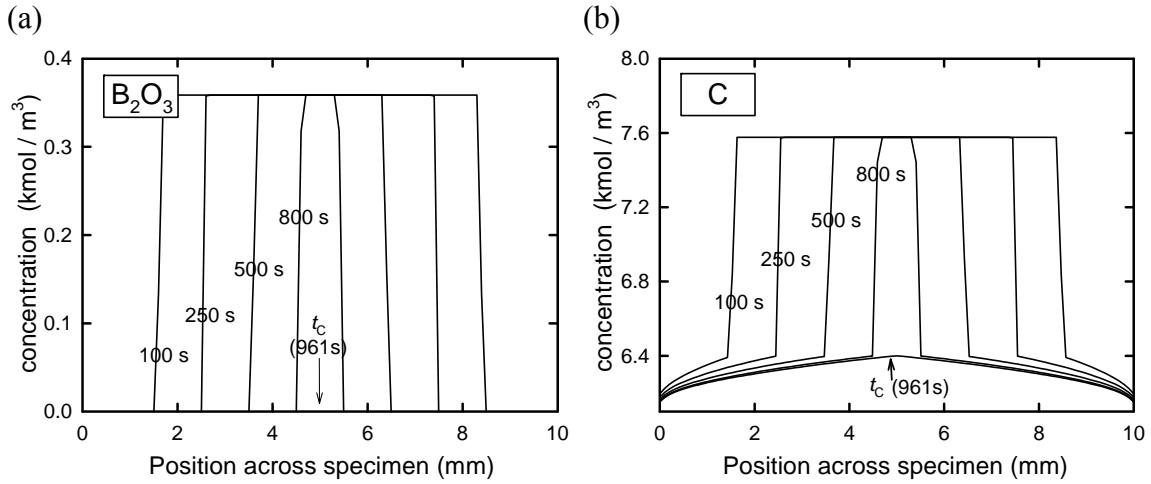
**Fig. 1:** Gas pressures as a function of temperature for several species in equilibrium with solid B<sub>4</sub>C, C and liquid ( $T > 723$  K) B<sub>2</sub>O<sub>3</sub>.



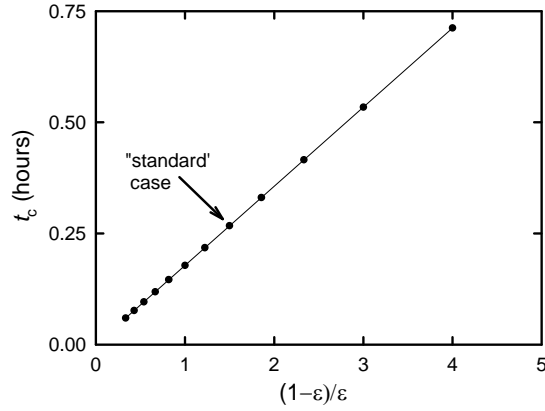
**Fig. 2:** (a) Partial pressure of CO as a function of position at several times and (b) as a function of time at several positions beneath the specimen surface.



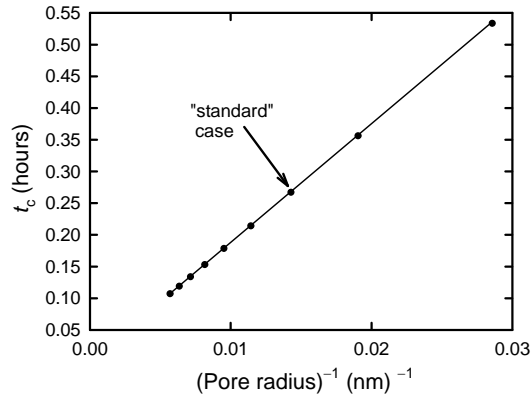
**Fig. 3:** Partial pressure profiles of the gaseous species (a)  $B_2O_2$ , (b)  $B_2O_3(g)$  and (c) BO as a function of position across the sample thickness at various times.



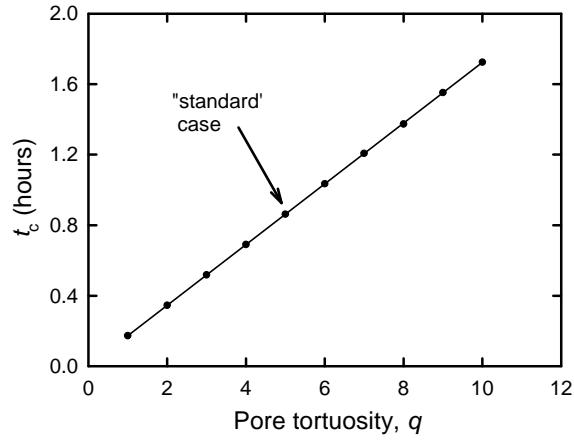
**Fig. 4** (a) The profile of  $B_2O_3$  (c) and (b) C as a function of position at various times during the temperature hold.



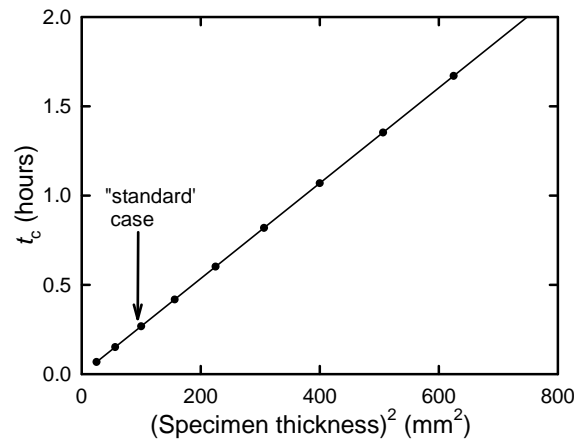
**Fig. 5:** Holding time for complete  $B_2O_3$ (c) removal as function of  $(1-\epsilon)/\epsilon$ .



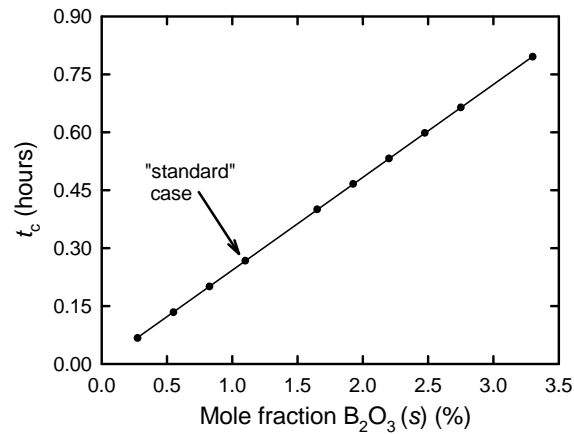
**Fig. 6:** The holding time required for the removal of  $B_2O_3$ (c), as a function of pore radius on a reciprocal scale.



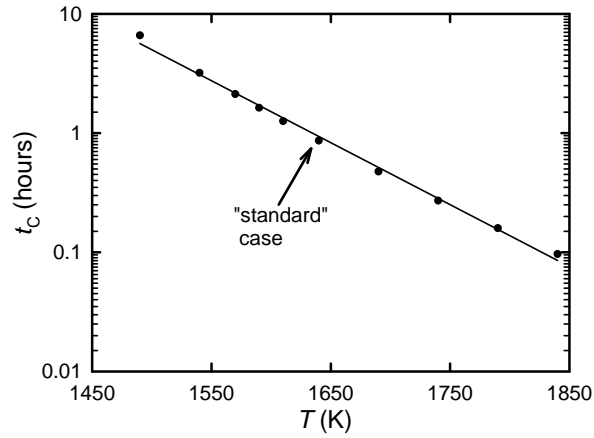
**Fig. 7:** The holding time required for the removal of  $B_2O_3(c)$ , as a function of pore tortuosity.



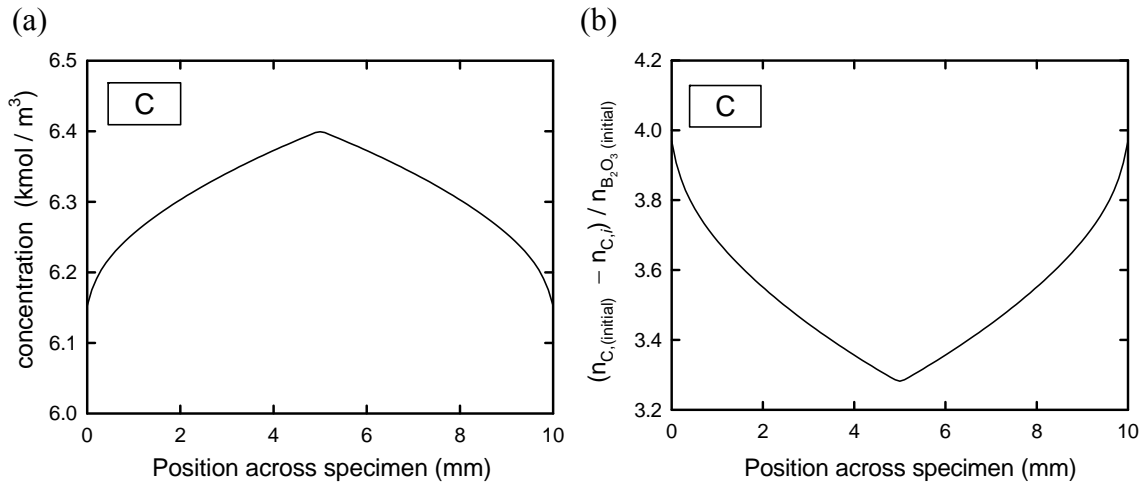
**Fig. 8:** The holding time required for the removal of  $B_2O_3(c)$ , as a function of the square of the specimen thickness



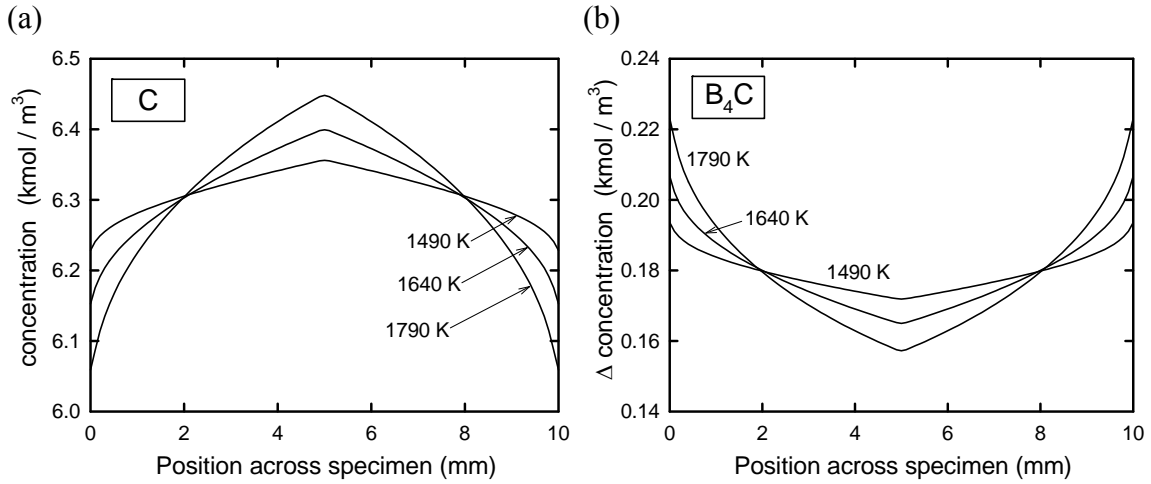
**Fig. 9:** Holding time as a function of initial  $B_2O_3(c)$  content in  $B_4C$  powder.



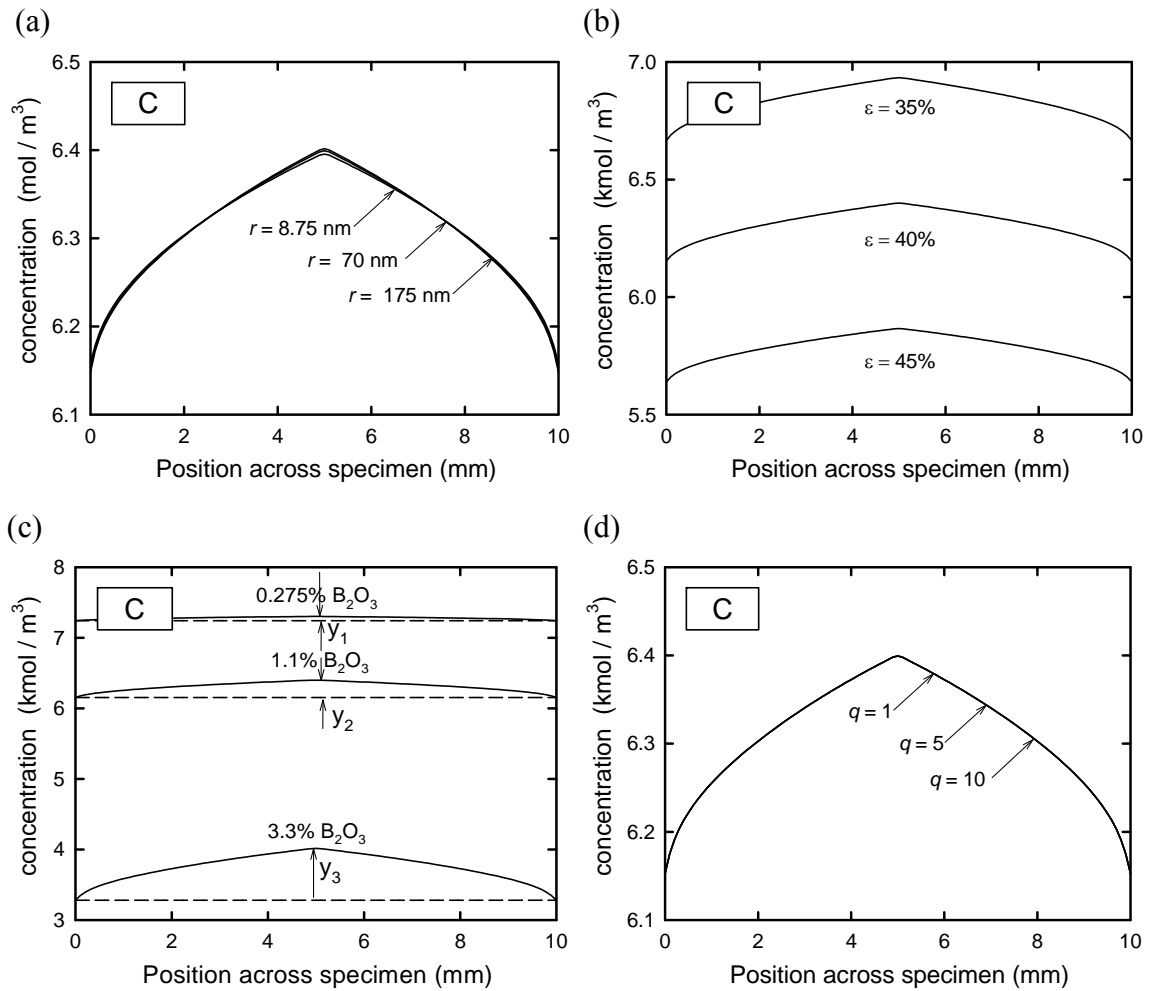
**Fig. 10:** Holding time required for the removal of  $B_2O_3(c)$ , as a function of temperature.



**Fig. 11:** (a) Residual C concentration profile after complete  $B_2O_3(c)$  depletion from specimen. (b) Change in number of moles of C normalized to the initial number of moles of  $B_2O_3(c)$ .



**Fig. 12:** (a) Residual C concentration profile at  $t_c$ , as a function of temperature ( $T$ ). (b) Change in  $\text{B}_4\text{C}$  concentration profile at  $t_c$ , as a function of temperature ( $T$ ).



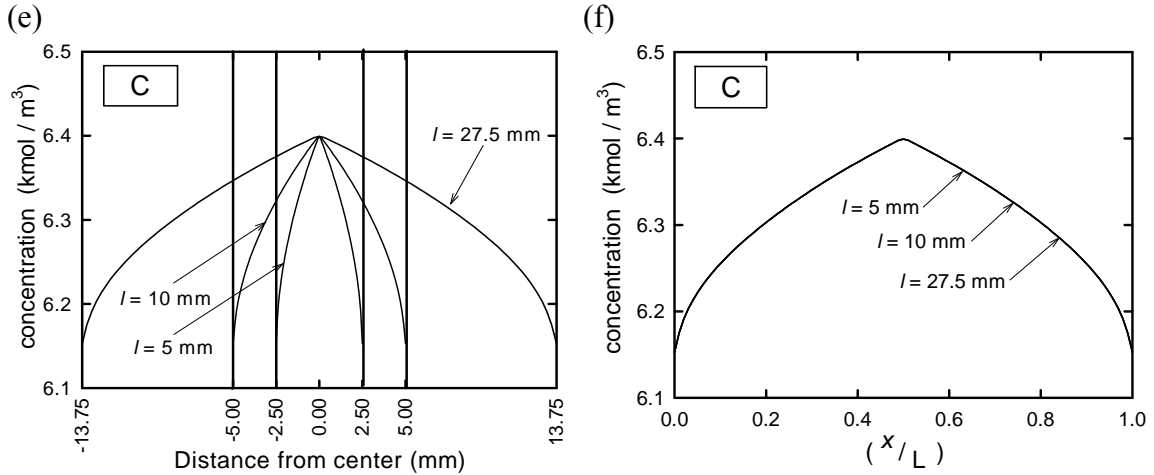


**Fig. 13:** Residual C concentration profile at  $t_c$  as a function of (a) pore radius  $r$ , (b) porosity  $\varepsilon$ , (c)  $X_{B_2O_3}$ , (d) tortuosity  $q$ , and (e) specimen thickness,  $l$ . (f) shows the data from (e) re-graphed as a function of position normalized to the overall specimen thickness.